Monthly Notices of the ROYAL ASTRONOMICAL SOCIETY

MNRAS **484,** 3620–3624 (2019) doi:10.1093/mnras/stz249
Advance Access publication 2019 January 23

First multiband atmospheric extinction in Antarctica PAIX monitoring the South Polar Sky

M. Chadid[1] and J. Vernin[2]★

[1]*University of Côte d'Azur, Artemis UMR 7250, F-06304 Nice Cedex 4, France*
[2]*TANGO – Tibet & Antarctica Network Ground Observatories, 107 Route de Saint Pierre de Féric, F-06000 Nice, France*

Accepted 2019 January 18. Received 2019 January 18; in original form 2018 October 10

ABSTRACT

For the first time, multiband atmospheric extinction in Antarctica is reported. Extinction coefficients are derived from 17 500 CCD stellar frames, by use of simultaneous multicolour Johnson–Cousin filters, over a whole polar wintertime. Polar observations were performed using PAIX – Photometer AntarctIca eXtinction, the first Antarctica robotic multiband photometer. Bouguer's lines and then the atmospheric extinction coefficients are inferred from 1.2 and 1.8 airmass continuous and uninterrupted observations of the same target. Besides the known good seeing, large isoplanatic angle, high coherence time, and exceptional light transmission in the whole IR-mm bandwidth, we detect that the blue atmospheric extinction at Dome C is 1.6–1.9 times better than that of the highest ranking ground-based observatories around the world. Moreover, our results show a similar atmospheric extinction value in the *V* band at Dome C and the ground-based observatories. However, in the *R* band, the atmospheric extinction coefficient is worse at Dome C than the ranking ground-based observatories. The original polar technology – PAIX – opens a new window towards novel insights in long-term time series stellar pulsation and evolution studies.

Key words: atmospheric effects – instrumentation: photometers – site testing – techniques: photometric.

1 INTRODUCTION

Dome C (75°03′S, 123°20′E) is located on one of the highest summits of the polar plateau in Antarctica, at an altitude of 3233 m, and temperature variations between −20° C in summertime and −80° C in wintertime. The extremely cold temperatures, whatever the relative humidity, insure a very low water vapour content (wvc is the thickness of condensed water in the air column above the site) of 0.52–0.64 mm at Dome C (Valenziano & Dall'Oglio 1999), 0.45 ± 0.25 mm throughout the year (Smythe & Jackson 1977) at the US Amundsen-Scott station, and 0.13 mm at Dome A (Sims et al. 2012) during the wintertime. These extremely low wvc values make the sites of high Antarctica plateau the best ground-based astronomical observatories for light transmission in the whole IR-mm bandwidth.

In the optical range, the number of clear nights is a major parameter. The duty cycle limited by meteorology is as high as 92 per cent [Mosser & Aristidi (2007), Trinquet et al. (2008) and by Aristidi et al. (2009)], better than 85 per cent encountered in the highest ranking ground-based astronomical sites. However, close to the geographic poles, day and night are less well defined and the amount of time when the sun is below some threshold, −18° for the astronomical twilight, has to be taken into account. According to the telescope aperture (*F*/*D* ratio), a lower threshold might be allowed, as demonstrated by Chadid et al. (2010), using the Photometer AntarctIca eXtinction (PAIX) photometer. From their photometric study, the images could be collected and processed even when the sun is at −8° below horizon. In this case, the accumulated observable time spans over approximately 136 d, and observation is possible without any interruption during 22 consecutive days.

One of the most important concerns for astronomical site qualification is the atmospheric extinction parameter which measures the magnitude loss per airmass (AM). As the line of path increases when the star sets on the horizon, and according to AM = 1/cos(z), where z is the zenith angle, the atmospheric absorption gets stronger, and then the apparent magnitude of the star increases. In a perfect case without the terrestrial atmosphere, the atmospheric extinction value is 0 mag am^{-1}.

PAIX, the first Antarctica robotic photometer (Chadid et al. 2016), gives an unprecedented atmospheric extinction measurement in Antarctica, in particular at Dome C. In this paper, we briefly describe PAIX and data analysis in Section 2, results and discussion in Section 3, and finally, some concluding remarks and perspective are given in Section 4.

★ E-mail: vernin@unice.fr

2 PAIX AND DATA ANALYSIS

2.1 Method of observation

Using PAIX, we observed, at different zenith angle, the circumpolar standard star, TYC 8120-550-1 ($\alpha = 7^{h}21'00\farcs54, \delta = -46°42'47\farcs1$), This star has been chosen according to Bouguer's line criteria (Bouguer 1729) that explain in fact, the target must be located far from the geographic pole, uninterruptedly observed and then permanently able to move up and down above the horizon in respect of a Bouguer's line setting up.

2.2 PAIX – first robotic Antarctica photometer

PAIX is the first robotic multiband photometer (Chadid et al. 2016), operational since 2007 and located at Dome C in the open field, without any shelter and installed at ice level. PAIX is attached to the Cassegrain focus of a 40-cm Ritchey–Chretien optical telescope, with an F/D ratio of 10, supported by an equatorial mount AstroPhysics 1200. At the focus are successively installed a robot-focus (Optec TCF), a filter wheel (SBIG-CFW6) equipped with Johnson–Cousin filters and a CCD dual chip (SBIG-ST10-XME), all included in a thermalized box. Collecting simultaneously multicolor light curves of several targets within the same 12.2 × 8.2 arcmin field of view, PAIX has been antarctized to run under extreme weather conditions with temperatures as low as −80 °C, and has been robotized, designed and built by the international PAIXTeam headed by Merieme Chadid.

All PAIX components are remotely controlled and setup through Paix ACquisition Software (PACS) implemented on PAIX experiment at Dome C, and accessible from anywhere through a virtual private network and a remote desktop.

The observing run started on 2011 May 12 and ended on 2011 September 25 collecting about 17 500 CCD images. From time to time, dark-flat-bias frames are recorded for further image processing and calibration. For each *BVR* photometric band, the exposure time is set to $\Delta t = 60$ s, and within the field of view (12.2 × 8.2 arcmin), hundreds stars are detected, among which the pulsating star HH Puppis for the astronomical purpose, and the reference star TYC 8120-550-1 for the extinction coefficient measurement. In order to show PAIX efficiency, Fig. 1 shows the 3D observed light curve behaviour of HH Puppis, a typical RR Lyrae star, folded with the pulsation period, throughout the three *BVR* colour filters, during 136 d of 2011 polar wintertime.

2.3 PAIX data processing pipeline

The pipeline software was established to process all 17 500 raw images. Each image is calibrated from dark-flat-bias correction and then hot pixels are swept away and replaced by an average of neighbour pixels. The pipeline uses astrometry.net[1] to recognize the field of view and yields $\{\alpha, \delta\}$ coordinates of the detected stars. Multiband photometry is performed with use of SExtractor[2] creating a catalogue of the whole stars in the image, providing their magnitude, error magnitude, and FWHM seeing in both *x*- and *y*-axis. The catalogue is analysed to find the reference star, towards the extinction coefficient measurements, and the target stars, in particular the pulsating variable stars towards astrophysical purposes (Chadid et al. 2014).

[1] http://nova.astrometry.net/
[2] http://www.astromatic.net/software/sextractor

3 RESULTS AND DISCUSSION

3.1 PAIX observations

Fig. 2 shows the Bouguer's line[3] from the different *BVR* colours, the slope refers to the extinction in mag am^{-1} unit. The equation of the line is determined with a linear fit, with the slope *A* in mag am^{-1}, the magnitude at origin *B*, i.e the absolute brightness outside the atmosphere and finally the correlation coefficient *R*, for the three different *BVR* colours. Fig. 2 demonstrates more measurements taken when the star is closer to horizon (high airmass) than to zenith (low airmass). To compensate, we divided the airmass range into 20 equal segments and then we established the mean, median, and dispersion magnitude values, given by vertical error bars. Then, a linear fit is calculated with the sub-set values. However, with or without this segmentation, the statistical regression gives the similar values of extinction, absolute magnitude, and correlation.

3.2 Modelling the observations

Fig. 3 shows the measured and modelled extinction coefficients in *BVR* bands at three different ground-based sites, Observatorio Roque de los Muchachos (ORM), Mauna Kea (MK), and Dome C. The atmospheric extinction value is given in mag am^{-1} unit.

The most publications on broad-band photometry take into account three major contributions: the Rayleigh scattering (black curve), the ozone absorption (red curve), and the aerosol absorption (cyan curve). The green curve is the sum of the three above mentioned contributions. Based on previous works (Hayes & Latham 1975), a model for each type of absorption is used to analyse our measurements. Among many articles on the atmospheric extinction, Mauna Kea site observations were interpreted with the same three contributions (Buton et al. 2013). The authors added a new extinction component due to telluric lines. In this paper, We will not take the telluric lines extinction into account.

Here we recall the three contributions to absorption (Hayes & Latham 1975):

(i) Rayleigh scattering: The extinction is given by

$$A_{\mathrm{Ray}}(\lambda, h, \mathrm{site}) = B_{\mathrm{Ray}}(\mathrm{site})\, 9.4977 \times 10^{-3} \left(\frac{1}{\lambda}\right)^4 \times \left[\frac{(n-1)_\lambda}{(n-1)_{\lambda=1}}\right]^2 \exp\left(\frac{-h}{7.996}\right), \quad (1)$$

where h is the altitude and the refractive index term is given by

$$\frac{(n-1)_\lambda}{(n-1)_{\lambda=1}} = 0.234\,56 + \frac{1.076 \times 10^{-2}}{145 - (1/\lambda)^2} + \frac{0.931\,61}{41 - (1/\lambda)^2}. \quad (2)$$

(ii) Ozone: The ozone absorption (Hayes & Latham 1975) refers to previous work (Howard 1960) along with coefficient in the ultraviolet and optical region (Inn & Tanaka 1953). We fitted the absorption coefficient versus wavelength curve of fig. 3 of the previous article to get a model in the region 0.4−0.75 μm with the following Gaussian equation:

$$A_{\mathrm{oz}}(\lambda, \mathrm{site}) = B_{\mathrm{oz}}(\mathrm{site})\, 0.055 \exp\left(-\frac{(\lambda - 0.59)^2}{0.0048}\right). \quad (3)$$

[3] Also known as Langley extrapolation.

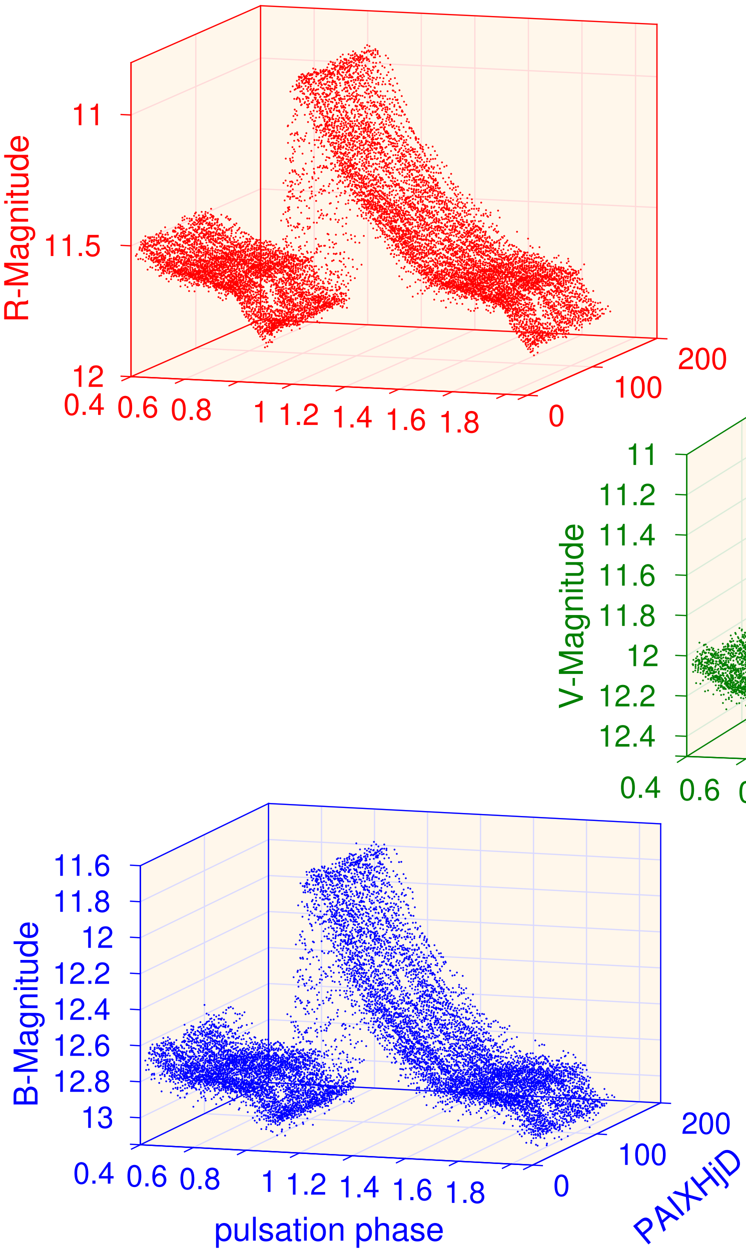

Figure 1. Three-dimensional observed PAIX light curve of RR Lyrae star HH Puppis folded with the pulsation period (0.390 d), in three *BVR* colours, during the observing run of 2011 polar wintertime. Axis refers to phase, magnitude, and PAIX Heliocentric Julian Day.

(iii) Aerosol scattering: Following Hayes & Latham (1975), aerosol scattering is given by

$$A_{\rm aer}(\lambda, h) = A_0\, \lambda^{-\alpha} \exp(-h/H) \quad (4)$$

but might be simplified, as proposed by Buton et al. (2013)

$$A_{\rm aer}(\lambda, h) = \tau\, \lambda^{-\mathring{a}} \quad (5)$$

and finally they adopt $\mathring{a} = 1$ and $\tau = 0.007$ is also adjustable to each site. For a given site the above equation might be rewritten as

$$A_{\rm aer}(\lambda, {\rm site}) = B_{\rm aer}({\rm site})\, 0.007\, \lambda^{-1}, \quad (6)$$

where $B_{\rm Ray}$(site), $B_{\rm oz}$(site), and $B_{\rm aer}$(site) are three adjustable coefficients used to fit the model with the experimental measurements. Rayleigh scattering arises from air molecules contained in a column above the site and depends mainly on its altitude. For Dome C the mean pressure is about 641 hPa which corresponds to an altitude of about 3700 m, higher than the geographical altitude $h = 3230$ m. This is due to the fact that Dome C is predominantly affected by low pressure, as noticed by Tomasi et al. (2011). The altitude of ORM and Mauna Kea are respectively 2200 and 4200 m. The Rayleigh adjustable parameter $B_{\rm Ray}$(site) was constrained within a ±10 per cent variation range to take into account the high dependence on altitude of the site. The two other parameters $B_{\rm oz}$(site) and $B_{\rm aer}$(site) where left to vary within a larger range.

Atmospheric extinction coefficients in the three *BVR* bands at ORM and MK are published in various publications as explained below.

(i) ORM: Most of the references are based on Carlsberg Meridian Circle (CAMC) data compared with theoretical model (King

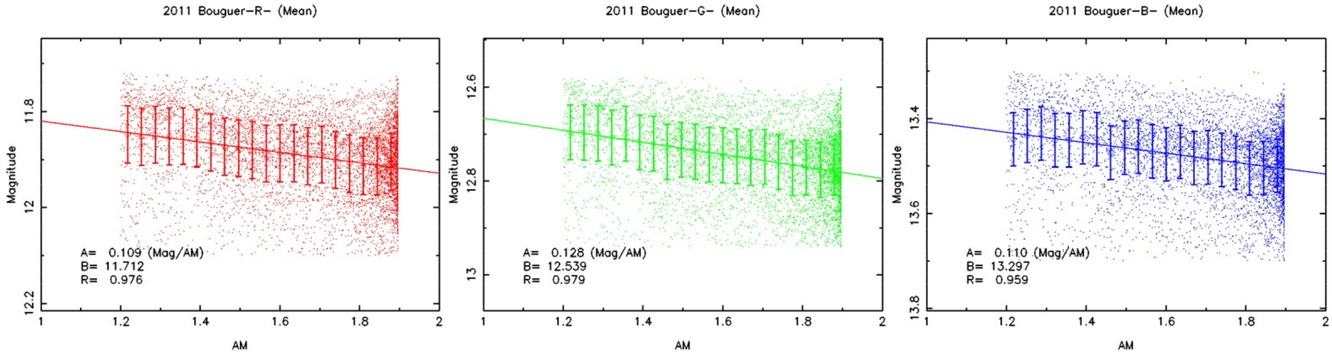

Figure 2. Bouguer's line through red, visible, and blue filters, from left to right. Slant lines correspond to the best linear fit whose slope yield the atmospheric extinction in magnitude per airmass. Vertical bars refer to the standard deviation of the magnitude dispersion within 20 airmass sub-ranges, scattered between 1.2 and 1.9. In each panel are given the slope A, the magnitude of the reference star outside the atmosphere B and the correlation coefficient R, for each colour.

[h]

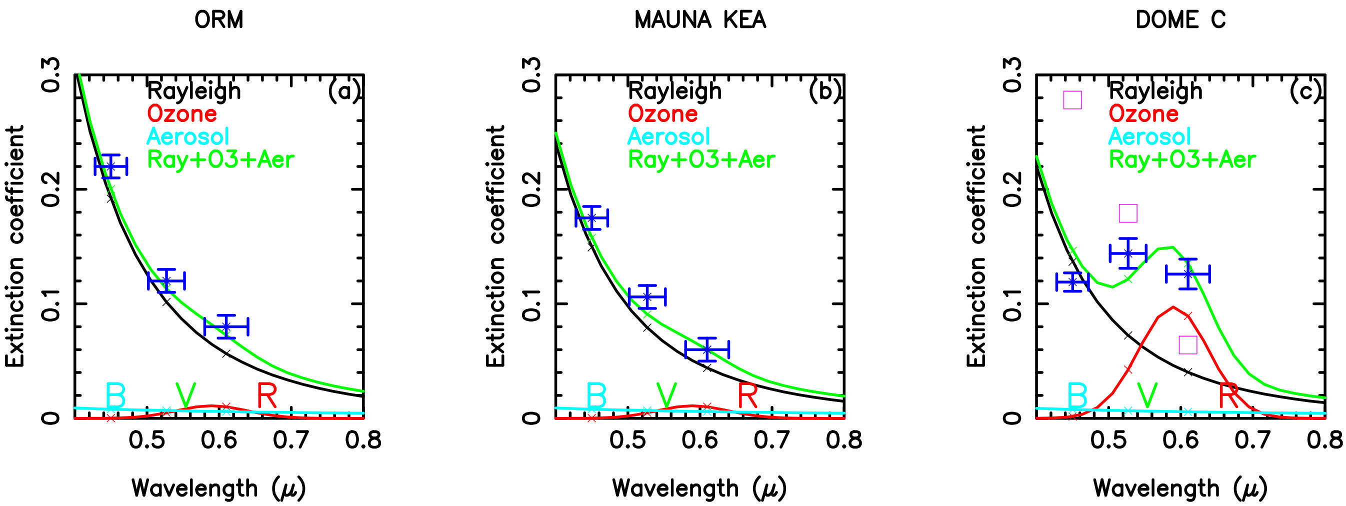

Figure 3. Atmospheric extinction (green line) at the three sites ORM (a), Mauna Kea (b), and Dome C (c), deduced from the respective contribution of the Rayleigh scattering (black line), ozone absorption (red line), and aerosol absorption (blue line). *B*, *V*, and *R* letters correspond to the respective wavelength centre in each filter band: 0.450, 0.527, and 0.610 μm. Blue + refers to measured atmospheric extinction.

1985) in the spectral range 300–1100 nm, using the same model (Hayes & Latham 1975). Then, in 2003, extinction coefficients in the *BVR* bands were deduced from Jacobus Kapteyn Telescope (Kidger et al. 2003). Finally in 2010, another extinction coefficient was published (García-Gil, Muñoz-Tuñón & Varela 2010).

(ii) Mauna Kea: Here we refer to a comprehensive study (Buton et al. 2013) which summarizes a number of previous publications made at Mauna Kea.

We enlarge the comparison between three additional sites: Cerro Paranal (Patat et al. 2011), Cerro Tololo (Gutierrez-Moreno, Cortes & Moreno 1982), and also a less known site Gaomeigu (Hu 2011; 3200 m) in China. Table 1 summarizes the comparison between the six ground-based astronomical sites. Our results from Dome C demonstrate that the atmospheric extinction value at Dome C is similar to the five ground-based astronomical sites, cited-above, in RV bands. However, in *B* band, the atmospheric extinction at Dome C outperforms the five sites by a factor of 1.6–1.9.

Fig. 3 shows that the curve of variation of extinction as a function of wavelength, that we call extinction curve, strongly varies from Dome C to the ORM and Mauna Kea sites. Instead of a permanent decrease, the extinction curve at Dome C shows a pronounced bump in the *R* and *V* bands, and a *B* extinction values lower than that of the ORM and Mauna Kea Sites.

Fig. 3(c) shows that at Dome C, the ozone absorption prevails within the 0.55–0.65 μm band. Dome C and Mauna Kea, the two high altitude sites, are affected by almost the same amount of

Table 1. Atmospheric extinction comparison, in *BVR* bands, between Dome C (this study), Observatorio Roque de los Muchachos (ORM), Mauna Kea (MK), Cerro Tololo, Cerro Paranal, and Gaomeigu. The third line *N* gives the number of CCD stellar frames used in this study.

Extinction λ (μm)	*R* filter 0.610	*V* filter 0.527	*B* filter 0.450
Dome C	0.109	0.128	**0.110**
N 17500	6100	5900	5500
ORM	0.094	0.120	0.220
MK	**0.060**	**0.106**	0.175
Tololo	**0.060**	0.140	0.210
Paranal	0.068	0.116	0.211
Gaomeigu	0.142	0.198	0.336

Rayleigh scattering, less than ORM, in the three *BVR* bands. The aerosol absorption is low and very similar at all the three sites.

4 CONCLUSIONS AND PERSPECTIVE

For the first time, we report an exceptional blue atmospheric extinction from a ground-based astronomical site. These unprecedented results are remarkable and the most striking result shows that the light at the shorter wavelengths is less absorbed by the earth's atmosphere at Dome C. That is a first essential step towards a new polar astronomy and deserves a renewed investigation of ultraviolet band atmospheric extinction measurements at Dome C that might be undertaken. A dedicated telescope brings new insights on the ultraviolet Universe, in the late stages of its evolution by (1) measuring the temperature, densities, and chemical composition of hot young stars and the interstellar medium, (2) providing crucial information about the evolution and structure of galaxies, and finally, (3) detecting the signature of higher energy radiation of hotter objects, typically in the early and late stages of their evolution and also young massive stars near their birth or death towards determining the primordial deuterium remaining from the big bang.

Finally, in order to overcome the optical turbulence and attain the high angular resolution – using adaptive optics – all of the last generation of telescopes observes in the IR-micron band. Therefore, we stress the need of a new generation of telescopes, installed 20–30 m above the ice level at Dome C to attain a better angular accuracy in *BVR* bands, with a seeing dropping to 0.3–0.4 or even 0.27 arcsec [Lawrence et al. (2004) and Giordano et al. (2012)] towards an exceptional transparency in the optical *B* band. This means that such telescopes will compete with space missions and even overtake them in term of observation flexibility, failure repair, and finally the inexorable space high costs.

ACKNOWLEDGEMENTS

The PAIX project is supported by the United States Air Force Research Laboratory through its European Office of Aerospace Research and Development, the French Agence Nationale de la Recherche (ANR-05-BLAN-0033-01), the French and Italian Antarctic Research Programs, IPEV and PNRA, the Conseil des Programmes Scientifiques et Technologiques (CPST), and the Programme National de Physique Stellaire (PNPS). Special thanks are addressed to the polar Institut Paul Emile Victor (IPEV) for the valuable and ongoing help. We are indebted to all polar staffs who participate to PAIX Antarctic expeditions. Finally, we notably thank the PAIX Team for his continued and strong dedication to the PAIX project.

REFERENCES

Aristidi E. et al., 2009, A&A, 499, 955
Bouguer P., 1729, Essai d'Optique sur la Gradation de la Lumière
Buton C. et al., 2013, A&A, 549, A8
Chadid M., Vernin J., Mekarnia D., Chapellier E., Trinquet H., Bono G., 2010, A&A, 516, L15
Chadid M. et al., 2014, AJ, 148, 88
Chadid M. et al., 2016, Evans C. J., Simard L., Takami H., in Ground-based and Airborne Instrumentation for Astronomy VI. SPIE, Bellingham, p. 99080
García-Gil A., Muñoz-Tuñón C., Varela A. M., 2010, PASP, 122, 1109
Giordano C., Vernin J., Chadid M., Aristidi E., Agabi A., Trinquet H., 2012, PASP, 124, 494
Gutierrez-Moreno A., Cortes G., Moreno H., 1982, PASP, 94, 722
Hayes D. S., Latham D. W., 1975, ApJ, 197, 593
Howard N. E., 1960, Handbook of Geophysics
Hu B., 2011, Chin. Astron. Astrophys., 35, 199
Inn E. C. Y., Tanaka Y., 1953, J. Opt. Soc. Am., 43, 870
Kidger M. R., Fabiola M.-L., Narbutis D., Perez-Garcia A., 2003, The Observatory, 123, 145
King D. L., 1985, RGO/La Palma technical note no 31
Lawrence J. S., Ashley M. C. B., Tokovinin A., Travouillon T., 2004, Nature, 431, 278
Mosser B., Aristidi E., 2007, PASP, 119, 127
Patat F. et al., 2011, A&A, 527, A91
Sims G. et al., 2012, PASP, 124, 74
Smythe W. D., Jackson B. V., 1977, Appl. Opt., 16, 2041
Tomasi C., Petkov B., Benedetti E., Valenziano L., Vitale V., 2011, J. Geophys. Res. (Atmos.), 116, D15304
Trinquet H., Agabi A., Vernin J., Azouit M., Aristidi E., Fossat E., 2008, PASP, 120, 203
Valenziano L., Dall'Oglio G., 1999, PASA, 16, 167

This paper has been typeset from a TEX/LATEX file prepared by the author.